Journal of Solid State Chemistry **160,** 8–12 (2001)
doi:10.1006/jssc.2001.9229, available online at http://www.idealibrary.com on IDEAL®

RAPID COMMUNICATION

Space Group and Structure for the Perovskite $Ca_{0.5}Sr_{0.5}TiO_3$

C. J. Howard[1]

Australian Nuclear Science and Technology Organisation, Private Mail Bag 1, Menai, New South Wales 2234, Australia

R. L. Withers

Research School of Chemistry, Australian National University, Canberra, Australian Capital Territory 0200, Australia

and

B. J. Kennedy

School of Chemistry, The University of Sydney, Sydney, New South Wales 2006, Australia

Received February 5, 2001; in revised form April 8, 2001; accepted April 30, 2001; published online June 29, 2001

Powder diffraction patterns from $Ca_{1-x}Sr_xTiO_3$, at $x = 0.5$, show superlattice peaks indicative of both *R*-($q = \frac{1}{2}[111]^*_p$) and *M*-($q = \frac{1}{2}[110]^*_p$) point octahedral tilting, though the metric is pseudo-tetragonal and indeed very nearly cubic. In a previous study [C. J. Ball, B. D. Begg, D. J. Cookson, G. J. Thorogood, and E. R. Vance, *J. Solid State Chem.* 139, 238–247 (1998)] this pseudo-tetragonal structure was assigned to space group *Cmcm* (orthorhombic) rather than to space group *Pnma*, the accepted space group for the structure of $CaTiO_3$. These two space groups are, however, very difficult to distinguish by powder diffraction techniques. Electron diffraction has been used to obtain diffraction patterns from single domain regions and by such means it has been established unequivocally that the space group at room temperature is not *Cmcm* but *Pnma*. © 2001 Academic Press

Key Words: **perovskite; space group; electron diffraction; structure; neutron powder diffraction.**

INTRODUCTION

The perovskites, nominal composition ABX_3, constitute a family of phases characterized by inherent structural flexibility, and the occurrence of temperature- or composition-induced phase transitions between subtly different structural variants (1). They attract considerable attention because of their technological applications (2), often associated with the phase transitions, and their importance in the earth sciences (3). The mineral perovskite itself, $CaTiO_3$, is a major component of Synroc (4), a synthetic rock form designed for the immobilization of radioactive waste.

The structural variation between various perovskite-related derivative structures is often so subtle that it can be difficult to distinguish and identify the different perovskite variants, especially when these show only slight departure from the cubic symmetry of the ideal (aristotype) structure. A case in point has been encountered in the system $Ca_{1-x}Sr_xTiO_3$ at compositions near $x = 0.5$. Recently, motivated by the role played by $CaTiO_3$ in Synroc as the host for fission product strontium, Ball, Begg, Cookson, Thorogood, and Vance (5) reported a rather detailed study of this system using synchrotron X-ray powder diffraction. The various phases were identified, and their space groups assigned, from the splitting or otherwise of the main perovskite peaks, and from the appearance of weak superlattice peaks associated with octahedral tilting and the concomitant multiplication of the parent unit cell.

The diffractometer used by Ball *et al.*, an evacuated 1.15-m-diameter Debye–Scherrer camera installed at the Australian National Beamline Facility at the Photon Factory in Tsukuba, Japan (6), gives excellent performance in both resolution and signal to noise, so superlattice peaks which might escape observation on a laboratory diffractometer can be quite readily seen. The main results and conclusions from the study, related to room temperature structures, were as follows: The end member $CaTiO_3$ is orthorhombic in *Pnma* is accord with earlier determinations (7). This is the

[1] To whom correspondence should be addressed. Fax: + 61 2 9543 7179. E-mail: cjh@ansto.gov.au.

0022-4596/01 $35.00

structure of compositions to about $x = 0.4$. Though all the superlattice lines persist beyond this value of x, the *Pnma* lattice parameters converge at about $x = 0.45$ to give a pseudo-tetragonal metric. This convergence has quite reasonably been taken to imply a change in symmetry, and Ball *et al*. suggest the space group for the composition range $x = 0.45$ to $x = 0.6$, where the structure is pseudo-tetragonal, may be *Bmmb* (a nonstandard setting of *Cmcm*). The structure from $x = 0.65$ to $x = 0.9$ is tetragonal in space group $I4/mcm$, indicated by the disappearance of certain of the superlattice reflections (corresponding to *M*-point distortions; see later) together with the sudden development of significant tetragonal splitting. The *R*-point reflections become weaker, and the tetragonal splitting diminishes, until at $x = 0.95$ the structure becomes cubic in $Pm\bar{3}m$, this also being the structure of the end member $SrTiO_3$ (8).

Neutron and laboratory X-ray powder diffraction studies of $Ca_{1-x}Sr_xTiO_3$ have also been reported by Pandey and co-workers (9, 10). The neutron patterns were scanned for superlattice peaks (these, being dependent mainly on oxygen displacement, are relatively stronger in neutron than in X-ray diffraction patterns), and the X-ray patterns were examined for peak splittings. The experimental results, with regard to both superlattice peaks and peak splitting, were entirely consistent with those reported by Ball *et al*. (5). Another laboratory X-ray diffraction study was reported very recently by Qin, Becerro, Seifert, Gottsman, and Jiang (11). But for the admitted difficulty in observing all the superlattice reflections, the results were again consistent with those of Ball *et al*. (5), particularly in the convergence of the *Pnma* lattice parameters near $x = 0.4$. The authors conclude [in agreement with (5)] that the most likely sequence in $Ca_{1-x}Sr_xTiO_3$ is *Pnma*, *Cmcm*, $I4/mcm$, and $Pm\bar{3}m$, the transitions occurring at about $x = 0.45$, $x = 0.65$, and $x = 0.92$. Carpenter, Becerro, and Seifert (12) have reviewed these and earlier measurements on $Ca_{1-x}Sr_xTiO_3$, with particular attention to the variation of lattice parameter(s) with composition.

The focus of the present study is the structure of the pseudo-tetragonal phase, and in particular the structure at composition $x = 0.5$. Ball *et al*. (5) suggested space group *Cmcm* on the basis of its pseudo-tetragonal symmetry (as contrasted with the orthorhombic symmetry at smaller x), yet the true symmetry of *Cmcm*, like that of *Pnma*, is orthorhombic. The structure in *Cmcm*, like that in *Pnma*, accounts for the superlattice reflections observed. In fact, the structure in *Cmcm* allows some reflections forbidden in *Pnma* (5), but these would be expected to be even weaker than the other superlattice reflections and are not observed. The assignment of space group *Cmcm* corresponds with that made for a pseudo-tetragonal phase, intermediate between *Pnma* and $I4/mcm$, in a study of the temperature-induced phase transitions in $SrZrO_3$ (13). In the course of our own studies of the high-temperature phase transitions in perovskites, we have suggested the occurrence of an analogous *Cmcm* intermediate phase in both $CaTiO_3$ (14) and $SrHfO_3$ (15). Yet there are problems with this assignment. First, from the group theoretical analysis of the transitions in perovskites (16), there seems to be no particular reason for a transition from the *Pnma* structure to that in *Cmcm*, and such a transition, if it did occur, could not be continuous. There is scant evidence for discontinuity at this transition either in the composition-mediated sequence of Ball *et al*. (5), or in the high-temperature sequences where we have suggested the *Cmcm* might occur (14, 15). Second, there has been no sign even in neutron powder diffraction patterns (14, 15) of the additional allowed reflections that would confirm the space group as *Cmcm*. Finally, we have shown in a recent very high-resolution neutron study (17) that the space group for the intermediate pseudo-tetragonal phase in $SrZrO_3$ is not *Cmcm* but rather *Imma*.

The difficulty of distinguishing *Pnma* from *Cmcm* by X-ray powder diffraction was clearly acknowledged by Ball *et al*. (5). There may be some possibility that the few peaks distinguishing the two space groups would be more easily observed using neutron powder diffraction, but in our own neutron diffraction measurements from $Ca_{0.5}Sr_{0.5}TiO_3$, some of which are reported in this paper, we have never observed the peaks which would prove the *Cmcm*. It was hoped that the structures might be distinguished by Rietveld method fitting to the neutron powder diffraction patterns, but fits of similarly good quality were obtained regardless of which structure was assumed. As noted by Ball *et al*., the structures could be quite readily distinguished if diffraction patterns from monodomain single crystals could be obtained. We have achieved this using electron beam microdiffraction, and by this means have established unequivocally that the space group is *Pnma*.

EXPERIMENTAL

The samples used in this work were from the batches prepared, via an alkoxide route, by Ball *et al*. (5), and the details of the preparation are given in that earlier reference. The samples used for neutron diffraction were pellets, about 8 mm diameter by 10 mm high, produced in the final firing. The samples for selected area electron diffraction, like those studied by X-ray diffraction, were obtained by grinding the pellets to a fine powder.

The neutron diffraction pattern shown in this paper was recorded at room temperature using the high-intensity power diffractometer, Polaris (18), at the UK pulsed spallation neutron source ISIS, Rutherford Appleton Laboratory. The aim was to record a pattern with very good statistics, suitable for analysis by the Rietveld method, and more particularly to give the best possible chance of observing those superlattice reflections which would confirm *Cmcm*

[those indexed *hhk*, *h* odd, *k* even, on the *Cmcm* unit cell, see Ref. (5)].

Three pellets of sample were loaded into an 11-mm-diameter vanadium sample can, and data collected for more than 12 hours (2215 μA h proton beam on the target), giving the intensity at the strongest peak to a statistical accuracy of about 0.2%. Data were recorded in all of the Polaris detector banks, those from both the high-resolution backscattering (145°) and low-angle (35°) detector bank being used in the analysis. After initial subtraction of an instrumental background, the Polaris data were normalized using an incident spectrum (and variation of detector efficiency with wavelength) derived from the measurement of incoherent scattering from a vanadium rod.

The samples for electron diffraction were, as mentioned above, obtained by grinding the pellets to a fine powder. The finely ground powder sample was dispersed onto a holey carbon film for the observations. Electron diffraction patterns (EDPs) were obtained by using a Philips EM 430 transmission electron microscope (TEM) operating at 300 kV. Typical areas illuminated were 0.5 μm in selected area mode, and 500–1000 Å in microdiffraction mode. Prior consideration of the symmetries and reflection conditions in space groups *Cmcm* (unit cell approximately $2a_p \times 2a_p \times 2a_p$, where a_p is lattice parameter of parent) and *Pnma* (unit cell approximately $\sqrt{2}a_p \times 2a_p \times \sqrt{2}a_p$) led us to conclude that the easiest way to distinguish the two structures would be to investigate the various different $\langle 110 \rangle_p$ type zone axis EDPs. The subscript again indicates reference to the parent unit cell. Briefly, the majority of such zone axis EDPs should show only $\mathbf{G}_p \pm \frac{1}{2}\langle 111 \rangle_p^*$ superlattice reflections. In the case of *Cmcm*, two (of six) such zone axis EDPs would show $\mathbf{G}_p \pm \frac{1}{2}\langle 110 \rangle_p^*$ and $\mathbf{G}_p \pm \frac{1}{2}\langle 001 \rangle_p^*$ superlattice reflections in addition to the $\mathbf{G}_p \pm \frac{1}{2}\langle 111 \rangle_p^*$ type reflections, whereas in the case of *Pnma* there exists a unique $\langle 110 \rangle_p$ type zone axis, the [001] in *Pnma*, in which only $\mathbf{G}_p \pm \frac{1}{2}\langle 001 \rangle_p^*$ superlattice reflections should occur. With indexing on the *Pnma* unit cell, this [001] zone axis EDP shows *hk*0 reflections, and the distinctive pattern of spots in this EDP arises from the reflection conditions *hk*0, *h* even and 0*k*0, *k* even (see Fig. 2 below). Observation of this distinctive EDP distinguishes unequivocally between space groups *Pnma* and *Cmcm*.

RESULTS AND DISCUSSION

The neutron diffraction pattern from $Ca_{0.5}Sr_{0.5}TiO_3$ as recorded in the backscattering detector bank is shown in part, that is for *d*-spacings from 1.6 to 2.4 Å, in Fig. 1. The main perovskite peaks have been indexed on the parent unit cell; none show any splitting at the resolution of this measurement, indicating that the metric is nearly cubic. The superlattice peaks have been marked according to their origin, from *R*-point distortions (TiO_6 octahedra in successive layers tilting in opposite sense, the reflections having half-integral indices on the parent unit cell), *M*-point distortions (octahedra in successive layers tilting in the same sense, reflections having one integral and two half-integral indices), or *X*-point distortions (occurring when *R*- and *M*-point distortions operate in concert). The reader is referred to the literature (16, 17) and especially to the work of Glazer (19, 20) for a more detailed discussion. The superscripts + and − of the Glazer notation are associated with *M*- and *R*-point distortions, respectively. As correctly argued by Ball *et al.* (5), the presence of *M*-, *R*-, and *X*-point superlattice peaks rules out the tetragonal structures [see Ref. (16)], except possibly that in $P4_2/nmc$, and also rules out space group *Imma* recently established for the pseudo-tetragonal intermediate structure in $SrZrO_3$ (16). We are thus in agreement with Ball *et al.* that the most likely structures are those in *Pnma* and *Cmcm*. We have marked in Fig. 1 where we might expect to observe the *hhk*, *h* odd, *k* even, reflections (indexing on the *Cmcm* cell) which would prove the structure in *Cmcm*; we see no evidence of any intensity in these positions. The pattern in Fig. 1 shows weak peaks not associated with the perovskite structure, but identified as being due to just under 1% by weight of TiO_2 rutile impurity.

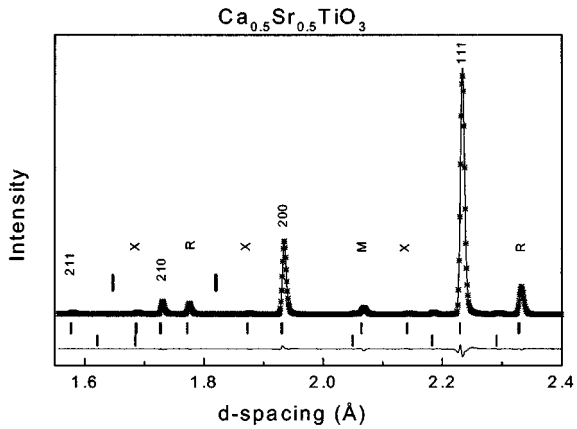

FIG. 1. Part of the neutron diffraction pattern from $Ca_{0.5}Sr_{0.5}TiO_3$ as recorded in the Polaris backscattering detector bank. The crosses represent the observed data, and the continuous line the least-squares (Rietveld) fit obtained, assuming the perovskite structure in *Pnma*. The rows of markers (vertical bars) below the pattern represent the calculated peak positions for the perovskite (upper) and the TiO_2 impurity (lower), and the two markers just above the diffraction trace indicate where additional peaks might be expected were the space group *Cmcm*. The main perovskite peaks have been indexed on the parent unit cell, and the superlattice peaks are marked according to the distortion from which they arise (see text).

The GSAS computer program (21) has been used to fit the neutron diffraction data from both backscattering and low-angle detector banks over the *d*-spacing ranges from 0.4 to 2.8 Å and 0.6 to 6 Å, respectively, assuming in turn the *Pnma* and *Cmcm* perovskite structures, and including TiO_2 rutile

as a second phase. The fit obtained assuming the *Pnma* structure is shown in Fig. 1, but the fit obtained assuming the *Cmcm* structure is of similar quality, so this Rietveld method approach cannot distinguish the two structures. Crystal structure parameters were refined in each case, and the results used in EDP calculations as explained below. The results for the *Pnma* structure (which we will show to be the correct choice) are recorded in Table 1.

Though the structures in *Pnma* and *Cmcm* may be difficult or impossible to distinguish by powder diffraction techniques, the structures are most certainly different. The details of these structures, as obtained by refinement from

TABLE 1
Structural Parameters for $Ca_{0.5}Sr_{0.5}TiO_3$

Atom	Site	x	y	z	B (Å^2)
Ca/Sr	4*c*	0.5126(1)	$\frac{1}{4}$	−0.0010(10)	0.92(2)
Ti	4*a*	0	0	0	0.54(1)
O1	4*c*	−0.0052(2)	$\frac{1}{4}$	−0.0501(2)	0.99(2)
O2	8*d*	0.2723(1)	0.0244(1)	0.2271(1)	0.99(2)

Note. Space group *Pnma*, $a = 5.4725(1)$, $b = 7.7324(1)$ and $c = 5.4715(1)$ Å. The numbers in parentheses indicate standard deviations, in units of the least significant figure, as estimated in the GSAS computer program.

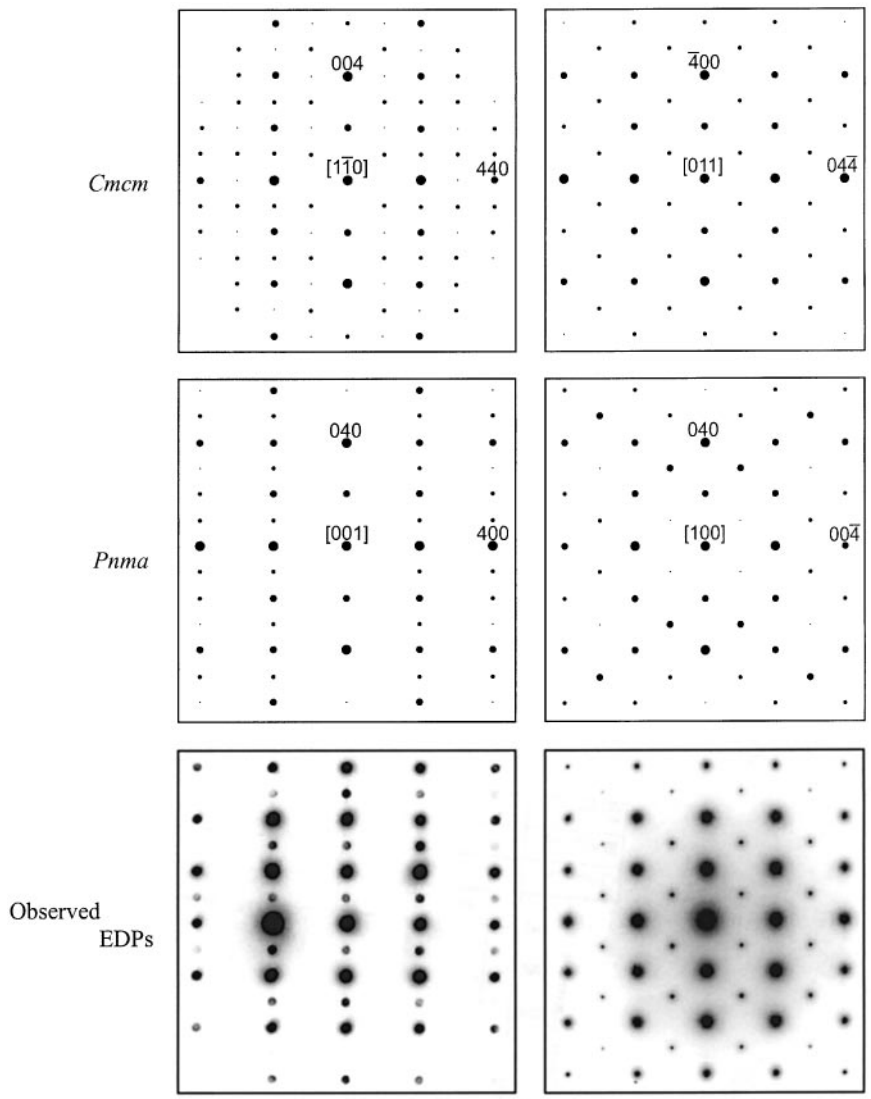

FIG. 2. Observed and calculated electron diffraction patterns (EDPs) from $Ca_{0.5}Sr_{0.5}TiO_3$. The $\langle 110\rangle_p$ type zone axis EDPs have been calculated assuming in turn the (neutron) structures in *Cmcm* and *Pnma*. Two distinctly different patterns are obtained in each case. By comparing the observed $\langle 110\rangle_p$ type zone axis EDPs (at bottom of figure) with the calculated ones (above), the space group is established beyond doubt as *Pnma*. The pattern shown on the right-hand side might not be a [100] zone axis pattern as indicated, but a $\langle 111\rangle$ zone axis pattern. The indexing of the left-hand pattern is, however, unambiguous, and it is the observation of this pattern that establishes the space group. The *Pnma* 0*k*0, *k* odd, reflections, missing (forbidden) from the calculated pattern, but appearing in the corresponding observed EDP, are the result of multiple scattering.

the neutron powder diffraction data, have been entered into Desktop Microscopist (Virtual Laboratories, P.O. Box 14266, Alberquerque NM 87191-4266), and the $\langle 110 \rangle_p$ type zone axis EDPs calculated in the kinematic approximation in each case. Calculated patterns are shown in Fig. 2, where they are also compared with patterns observed. The calculated EDPs show the general features anticipated earlier, in particular, the occurrence of a unique $\langle 110 \rangle_p$ type zone axis EDP, different from those occurring in *Cmcm*, that can be taken as a signature of the *Pnma*. The observed EDP shown on the left closely resembles the *Pnma* "signature" pattern, differing from it only through the appearance to superlattice reflections on the vertical row through the origin that are forbidden in *Pnma*. These reflections disappeared on tilting away from the zone axis, and were thus shown to be due to double diffraction. It is thus established beyond doubt that the perovskite $Ca_{0.5}Sr_{0.5}TiO_3$ has the *Pnma* structure, not that in *Cmcm*.

It has to be said that the EDPs shown in Fig. 2 were by no means the first $\langle 110 \rangle_p$ type zone axis EDPs observed. Patterns recorded using selected area electron diffraction showed superpositions in various proportions of the patterns of the left- and right-hand sides of Fig. 2, making it difficult to distinguish the space groups as required. These patterns evidently showed diffraction from more than one domain. The patterns shown in Fig. 2 were recorded using microdiffraction techniques, and would appear to represent diffraction from a single domain. (The pattern on the left is a clean *Pnma* [001] zone axis pattern; the pattern on the right is free from *Pnma* [001] zone axis contribution, but could contain contributions from more than one of the other $\langle 110 \rangle_p$ type zone axis EDPs.)

It has been argued above that the $\langle 110 \rangle_p$ type zone axis EDPs can be used to distinguish between the perovskite structures in *Pnma* and *Cmcm*. An examination of perovskite structures in the 15 possible space groups listed by Howard and Stokes (16) reveals no other $\langle 110 \rangle_p$ type zone axis EDP similar to the [001] zone axis pattern from the structure in *Pnma*. Thus, through our observation of this pattern, the *Pnma* structure is unequivocally established.

Given the result from this work, that $Ca_{0.5}Sr_{0.5}TiO_3$ has the *Pnma* structure, there is little reason to suppose that the *Cmcm* structure occurs in the $Ca_{1-x}Sr_xTiO_3$ system at any composition. It is thus quite likely that the sequence of structures is simply *Pnma*, *I*4/*mcm*, and $Pm\bar{3}m$. The first transition from *Pnma* to *I*4/*mcm*, occurring at about $x = 0.65$, would be necessarily discontinuous (16), though possibly volume conserving, and the second from *I*4/*mcm* to $Pm\bar{3}m$ occurring at about $x = 0.92$ would very likely be continuous. The reason for the high degree of pseudosymmetry of the *Pnma* structure in the range from $x = 0.45$ to $x = 0.65$ is not understood. There may be some possibility of an *Imma* phase intermediate between *Pnma* and *I*4/*mcm*, as occurs in the temperature-induced sequence for $SrZrO_3$ (17). It is difficult to comment on this on the basis of the published data, except to state that it could occur only for higher values of x. Neutron powder diffraction studies at elevated temperatures for compositions $x = 0.2$ and $x = 0.5$ (details to be published) suggest that the *Imma* might exist over a very narrow temperature range, but the occurrence of this possible intermediate is by no means definitely established.

ACKNOWLEDGMENTS

The authors thank Dr. Cliff Ball and Mr. Gordon Thorogood, ANSTO, for making available the sample of $Ca_{0.5}Sr_{0.5}TiO_3$ from the batches used in their earlier synchrotron X-ray powder diffraction studies (5), and Dr. David Mitchell, also from ANSTO, for assistance with the computer calculations of the electron diffraction patterns. The neutron diffraction pattern shown in this communication was recorded by Dr. Ron Smith from the ISIS facility, and Dr. Yasu Tabira of ANU assisted in recording the electron diffraction data. Support for travel of C.J.H. and B.J.K. from the Access to Major Research Facilities Program to undertake various X-ray and neutron diffraction measurements on this system is gratefully acknowledged. B.J.K. acknowledges support for his work on perovskites from the Australian Research Council.

REFERENCES

1. H. D. Megaw, "Crystal Structures—A Working Approach." W.B. Saunders, Philadelphia, 1973.
2. R. E. Newnham and G. R. Ruschau, *J. Am. Ceram. Soc.* **74,** 463 (1991).
3. A. E. Ringwood, *J. Geophys. Res.* **67,** 4005 (1962).
4. A. E. Ringwood, S. E. Kesson, K. D. Reeve, D. M. Levins, and E. J. Ramm, *in* "Radioactive Waste Forms for the Future" (W. Lutze and R. C. Ewing, Eds.), p. 233. Elsevier, Amsterdam, 1988.
5. C. J. Ball, B. D. Begg, D. J. Cookson, G. J. Thorogood, and E. R. Vance, *J. Solid State Chem.* **139,** 238 (1998).
6. T. M. Sabine, B. J. Kennedy, R. F. Garrett, G. J. Foran, and D. J. Cookson, *J. Appl. Crystallogr.* **28,** 513 (1995).
7. S. Sasaki, C. T. Prewitt, and J. D. Bass, *Acta Crystallogr., Sect. B* **43,** 1668 (1987).
8. R. H. Buttner and E. N. Maslen, *Acta Crystallogr., Sect. B* **48,** 639 (1992).
9. R. Ranjan, D. Pandey, V. Siruguri, P. S. Krishna, and S. K. Paranjpe, *J. Phys.: Condens. Matter* **11,** 2233 (1999).
10. R. Ranjan and D. Pandey, *J. Phys.: Condens. Matter* **11,** 2247 (1999).
11. S. Qin, A. I. Becerro, F. Seifert, J. Gottsman, and J. Jiang, *J. Mater. Chem.* **10,** 1609 (2000).
12. M. A. Carpenter, A. I. Becerro, and F. Seifert, *Am. Mineral.* **86,** 348 (2001).
13. M. Ahtee, A. M. Glazer, and A. W. Hewat, *Acta Crystallogr., Sect. B* **34,** 752 (1978).
14. B. J. Kennedy, C. J. Howard, and B. C. Chakoumakos, *J. Phys.: Condens. Matter* **11,** 1479 (1999).
15. B. J. Kennedy, C. J. Howard, and B. C. Chakoumakos, *Phys. Rev. B* **60,** 2972 (1999).
16. C. J. Howard and H. T. Stokes, *Acta Crystallogr., Sect. B* **54,** 782 (1998).
17. C. J. Howard, K. S. Knight, E. H. Kisi, and B. J. Kennedy, *J. Phys.: Condens. Matter* **12,** L677 (2000).
18. R. I. Smith, S. Hull, and A. R. Armstrong, *Mater. Sci. Forum* **166–169,** 251 (1994).
19. A. M. Glazer, *Acta Crystallogr., Sect. B* **28,** 3384 (1972).
20. A. M. Glazer, *Acta Crystallogr., Sect. A* **31,** 756 (1975).
21. A. C. Larson and R. B. Von Dreele, "GSAS General Structure Analysis System," Report LAUR 86-748. Los Alamos National Laboratory, Los Alamos, NM, 1986.